DOI: 10.1002/chem.201102066

Major Groove Substituents and Polymerase Recognition of a Class of Predominantly Hydrophobic Unnatural Base Pairs

Thomas Lavergne, Denis A. Malyshev, and Floyd E. Romesberg*[a]

Abstract: Expansion of the genetic alphabet with an unnatural base pair is a long-standing goal of synthetic biology. We have developed a class of unnatural base pairs, formed between d**5SICS** and analogues of d**MMO2** that are efficiently and selectively replicated by the Klenow fragment (Kf) DNA polymerase. In an effort to further characterize and optimize replication, we report the synthesis of five new d**MMO2** analogues bearing different substituents designed to be oriented into the developing major groove and an analysis of their insertion opposite d**5SICS** by Kf and *Thermus aquaticus* DNA polymerase I (Taq). We also expand the analysis of the previously optimized pair, d**NaM**–d**5SICS**, to include replication by Taq. Finally, the efficiency and fidelity of PCR amplification of the base pairs by Taq or Deep Vent polymerases was examined. The resulting structure–activity relationship data suggest that the major determinants of efficient replication are the minimization of desolvation effects and the introduction of favorable hydrophobic packing, and that Taq is more sensitive than Kf to structural changes. In addition, we identify an analogue (d**NMO1**) that is a better partner for d**5SICS** than any of the previously identified d**MMO2** analogues with the exception of d**NaM**. We also found that d**NaM**–d**5SICS** is replicated by both Kf and Taq with rates approaching those of a natural base pair.

Keywords: DNA · gene technology · Klenow fragment · polymerase chain reaction · Taq polymerase

Introduction

The four letter genetic alphabet is conserved throughout nature and is based on the complementary shape and hydrogen bonding (H bonding) of the natural purines and pyrimidines. For over two decades, efforts have been focused on the development of unnatural base pairs in which pairing is mediated by orthogonal H bonding patterns, and progress along this route continues.[1–4] However, we[5–16] and others,[17–21] have demonstrated that hydrophobic and packing forces are also sufficient to underlie the efficient and selective replication of an unnatural base pair. If sufficiently well replicated, such unnatural base pairs could be used as part of an expanded genetic system and would allow for an increase in the information potential of a genome, but will likely be useful immediately for in vitro applications, such as the site-specific labeling of enzymatically synthesized DNA or RNA with novel functionality (i.e., fluorophores or reactive moieties) for SELEX (systematic evolution of ligands by exponential enrichment)[22] or nanomaterial applications.[23]

Two of the most promising unnatural base pairs that we have identified are those formed by d**5SICS** and either d**MMO2** (d**MMO2**–d**5SICS**) or d**NaM** (d**NaM**–d**5SICS**; Figure 1a and b).[5,6,9,13,14] Previous studies with the Klenow fragment of *E. coli* DNA polymerase I (Kf) and T7 RNA polymerase have demonstrated that d**5SICS**–d**NaM** is replicated and transcribed with greater efficiency than d**MMO2**–d**5SICS**.[14] However, the d**MMO2** scaffold is simpler and more atom-economical than d**NaM**. In addition, the d**MMO2** scaffold provides more options for linker attach-

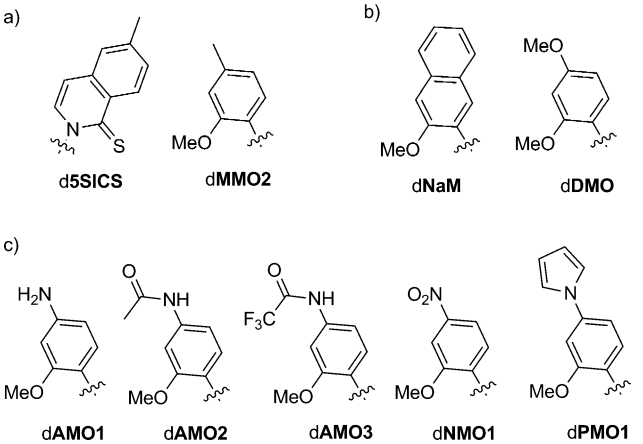

Figure 1. a) The d**MMO2**–d**5SICS** unnatural base pair; b) d**NaM** and d**DMO**; c) d**MMO2** analogues synthesized and evaluated in this study. Only nucleobase moieties are shown; sugar and phosphate backbone are omitted for clarity.

[a] Dr. T. Lavergne, D. A. Malyshev, Prof. Dr. F. E. Romesberg
Department of Chemistry, The Scripps Research Institute
10550 North Torrey Pines Road, La Jolla, California 92037 (USA)
Fax: (+1) 858-784-7472
E-mail: floyd@scripps.edu

Supporting information for this article is available on the WWW under http://dx.doi.org/10.1002/chem.201102066.

ment, which is required for site-specific labeling of the DNA, including attachment at the site analogous to that widely used with the natural pyrimidines[24] and not available with d**NaM**. Thus, our current efforts to expand the genetic alphabet include the continued evaluation of d**NaM**–d**5SICS**, with a particular focus on recognition by other polymerases that enable specific applications, such as PCR, as well as to continue to generate structure–activity relationship (SAR) data that will facilitate the further optimization of d**MMO2**–d**5SICS**.

A limiting step of replicating DNA containing d**MMO2**–d**5SICS** is the incorporation of d**MMO2**TP opposite d**5SICS**. Because existing SAR data suggest that this step is more sensitive to modifications of the triphosphate than of the templating nucleobase, we have focused on derivatizing d**MMO2**TP. The SAR data also clearly reveal that the *ortho* methoxy group is absolutely required for replication (the methyl group facilitates triphosphate insertion and the oxygen atom facilitates continued primer extension once the unnatural nucleotide is incorporated at the terminus[6]). In addition, the accumulated SAR data suggest that *para* derivatization is more promising than *meta* derivatization.[13,15] Initial efforts to identify beneficial modifications at the *para* position yielded d**DMO** (Figure 1b). While the d**DMO**–d**5SICS** unnatural base pair is replicated more efficiently than the parental d**MMO2**–d**5SICS** pair, it is still replicated less efficiently than d**NaM**–d**5SICS**.[8]

To continue our efforts to optimize the d**MMO2** scaffold, we now report the synthesis and characterization of five new derivatives bearing different moieties at the *para* position (Figure 1c). The specific modifications to the d**MMO2** scaffold were selected to systematically vary the size, shape, electronic properties, and H bonding potential of the nucleobase. The unnatural triphosphates were analyzed by determining the steady-state efficiencies with which they are inserted opposite d**5SICS** in a DNA template by Kf or by *Thermus aquaticus* DNA polymerase I (Taq). To further explore d**NaM**–d**5SICS**, we characterized its synthesis in both strand contexts (i.e., insertion of d**NaM**TP opposite d**5SICS** and d**5SICS**TP opposite d**NaM**) by Taq. To facilitate the detailed comparison of all the analogues in side-by-side experiments, the previously reported efficiencies of d**NaM**–d**5SICS** synthesis by Kf were redetermined, as were the insertion efficiencies of d**MMO2**TP and d**DMO**TP opposite d**5SICS** by Kf and Taq. Finally, each triphosphate was also analyzed by characterizing the PCR amplification of the corresponding unnatural base pair with d**5SICS** by Taq or Deep Vent polymerases. The results reveal important, and in some cases, polymerase-specific SAR data, and we found that d**NMO1**TP is better optimized than the other new analogues as a partner for d**5SICS**. The current analysis also reveals that d**NaM**–d**5SICS** is synthesized by Kf better than previously appreciated, and synthesized equally well by Taq, solidifying its position as the most promising unnatural base pair identified to date.

Results

Nucleotide design, synthesis, and evaluation: The unnatural nucleotides d**AMO1**, d**AMO2**, d**AMO3**, d**PMO1**, and d**NMO1** (Figure 1c) were designed to position different substituents in the developing major groove during replication. Each substituent was attached via a single bond to the position *para* to the glycosidic bond because SAR data suggest that rotational flexibility is important for efficient triphosphate incorporation[8] (although d**NaM** is an interesting and incompletely understood exception), presumably by allowing for the optimization of the developing interactions with d**5SICS** and/or the DNA polymerase. The simplest derivative of the series, d**AMO1**, bears only an amino substituent at the *para* position. In d**AMO2** and d**AMO3**, the amino moiety is modified with acetyl and trifluoroacetyl groups, which increase the size and reduce the ability of the substituent to donate electron density into the aromatic ring of the nucleobase scaffold. The nitro group of d**NMO1** is a potent electron withdrawing substituent. In contrast, incorporating the nitrogen atom within the context of the pyrrolo ring of d**PMO1** should have more modest electronic effects, but significantly increase the aromatic surface area of the scaffold.

The unnatural nucleotide derivatives were synthesized (Scheme 1). Briefly, the modified nucleoside **3** was obtained in three steps through Heck coupling between the 2′-deoxyribose glycal **1** and the appropriately iodinated *N*-Cbz-protected anisidine **2**, followed by deprotection of the sugar moiety and selective reduction of the resulting 3' keto group. Acceptable yields of the Heck coupling product required the use of an electron withdrawing group to protect the aromatic amine. The major coupling product was the desired β-anomer, confirmed by NOE experiments, which was separated from the minor α-anomer by silica gel column chromatography. The hydroxyl groups were simultaneously protected with tetraisopropyldisiloxane groups, and the Cbz group was removed by hydrogenation. Compound **4** was used as a common precursor to introduce diversity and access each of the desired nucleotides. We found that even under mildly acidic conditions, compound **4** is prone to epimerize to a mixture of α- and β-anomers, and careful control of all reaction conditions was required.

Toward d**NMO1**, the aromatic amine of **4** was first oxidized by using a potassium iodide-*tert*-butyl hydroperoxide catalyst, which cleanly converted the amine to the nitro group, whereas approaches based on in situ generation of the dimethyldioxirane or the use of methyltrioxorhenium/O_2 resulted in incomplete oxidation to the nitroso and hydroxylamine compounds, as well as the production of azoxy self coupled products. d**NMO1** (**5a**) was finally obtained by removal of the silyl protecting groups. Protected d**PMO1** was obtained by acid-free condensation[25] in aqueous 2,5-dimethoxytetrahydrofuran with microwave irradiation at 140 °C, which afforded the pure β-anomer, and the free nucleoside **5b** was obtained by removal of the silyl protecting group. Compounds **5c** and **5d** were obtained by acylation

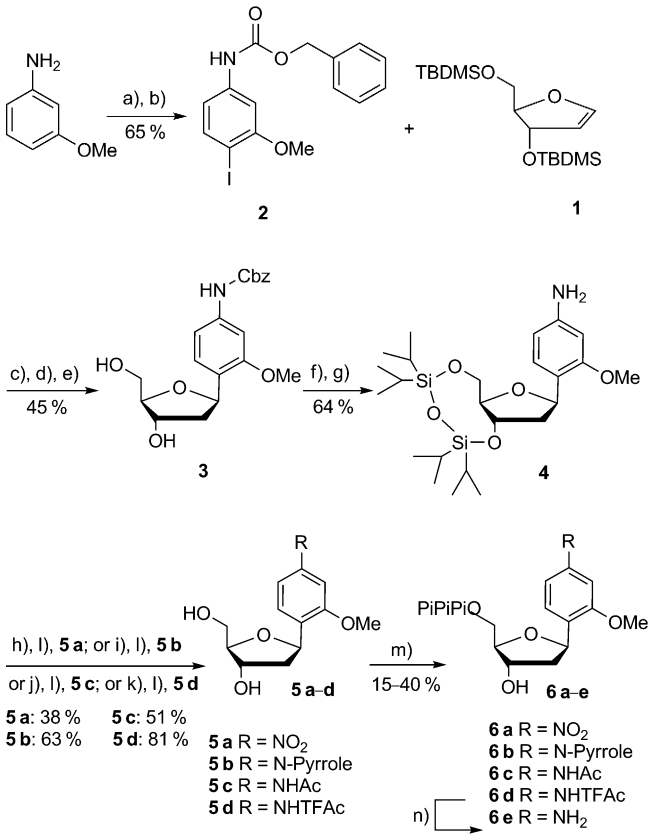

Scheme 1. Conditions: a) CBz-Cl, $NaHCO_3$, THF, room temperature, 20 min; b) I_2, Ag_2SO_4, MeOH, −20 °C, 1 h; c) $Pd(OAc)_2$, $AsPh_3$, nBu_3N, DMF, 70 °C, 15 h; d) TBAF 1 M in THF, 0 °C→room temperature, 2 h; e) $NaBH(OAc)_3$, AcOH, CH_3CN, 0 °C, 1 h; f) 1,3-dichloro-1,1,3,3-tetraisopropyldisiloxane, pyridine, room temperature, 2 h; g) 10 % Pd/C, H_2, EtOAc, room temperature, 1 h; h) KI, *t*-butyl hydroperoxide aq. 70 %, CH_3CN, dark, 75 °C, 2 h; i) 2,5-dimethoxytetrahydrofuran, H_2O, microwave 140 °C, 30 min; j) Ac_2O, Et_3N, CH_2Cl_2, room temperature, 20 min; k) trifluoroacetic anhydride, Et_3N, CH_2Cl_2, 10 °C, 20 min; l) TBAF 1 M in THF, 1 h; m) proton sponge, $POCl_3$, $PO(OMe)_3$, −15 °C→−10 °C, 3 h then Bu_3N, $(Bu_3NH)_2H_2P_2O_7$ in DMF, −10 °C→0 °C, 30 min then TEAB buffer (0.5 M), room temperature, 10 min; n) NH_4OH 30 %, room temperature, 1 h.

with acetic anhydride or trifluoroacetic anhydride, respectively, followed by TBAF-mediated sugar deprotection.

Free nucleosides **5a–d** were converted to the corresponding triphosphates **6a–d** by using Ludwig conditions,[26] and purified by anion exchange chromatography, followed by HPLC. d**AMO1**TP (**6e**) was obtained from d**AMO3**TP (**6d**) by ammonia-mediated deprotection of the amino group at room temperature. The purity of each triphosphate was confirmed by ^{31}P NMR spectroscopy, HPLC, and MALDI-ToF (see the Supporting Information). The triphosphates of d**MMO2**, d**DMO**, d**NaM** and d**5SICS** were prepared as described previously,[6,8,13] and the phosphoramidites of d**NaM** and d**5SICS** were prepared and incorporated into DNA as described previously.[13]

Each triphosphate was analyzed by examining its insertion opposite a correct or incorrect nucleotide in a DNA template by Kf and Taq under steady-state conditions, which provides a convenient assay to measure the overall rate at which product is formed.[27] The most interpretable data were the second order rate constant (or efficiency, k_{cat}/K_M) relating the duplex-bound polymerase and free triphosphate to the rate limiting transition state for the multiple turnover reaction. Assays with Kf were performed at 25 °C, which is close to the enzyme's optimal temperature of 37 °C. Because Taq is a thermophilic polymerase, assays with this enzyme were performed at 50 °C to allow for the use of the same primer–template substrates used with Kf and in previous studies. Although it is approximately 20 °C below optimum, Taq does retain a significant level of activity at this temperature.[28] Each analogue was also examined as a partner for d**5SICS** by PCR.

Efficiency of insertion of dMMO2TP, dDMOTP, and each natural dNTP opposite d5SICS: To gauge the efficiency of unnatural base pair synthesis, we first analyzed the insertion of dATP opposite dT in sequence context I (Table 1). In

Table 1. Kinetic data for Kf-mediated insertion of triphosphates (d**Y**TP) opposite d**5SICS** or d**NaM** in the template in sequence context I; insertion of dATP opposite dT is provided for comparison.

5′-d(TAATACGACTCACTATAGGGAGA)
3′-d(ATTATGCTGAGTGATATCCCTCT**X**GCTAGGTTACGGCAGGATCGC)

X	Y	k_{cat} [min^{-1}]	K_M [μM]	k_{cat}/K_M [$\times 10^5\,M^{-1}min^{-1}$]
T	A	4. 1±0.3	0. 0053±0.0004	7700
5SICS	**NaM**	14. 6±0.8	0. 25±0.04	580
	DMO	27. 0±1.5	12. 2±1.5	22
	MMO2	13. 7±2.0	35. 8±0.6	3.8
	NMO1	50. 1±8.8	22. 0±3.5	23
	PMO1	41. 7±6.7	20. 7±2.6	20
	AMO1	15. 3±3.5	178±62	0.86
	AMO3	13. 4±2.8	117±30	1.1
	AMO2	7. 0±1.0	464±100	0.15
	5SICS	12. 6±0.7	44. 2±11.7	2.9
	A	2. 1±0.3	52. 4±7.2	0.40
	G	11. 7±1.3	75. 5±3.7	1.5
	C	n.d.[a]	n.d.[a]	<0.01
	T	2. 1±0.4	230±11	0.091
NaM	**5SICS**	8. 3±1.1	0. 039±0.004	2100
	NaM	51. 5±3.4	5. 4±0.3	95
	A	24. 7±4.7	14. 0±0.8	18
	G	n.d.[a]	n.d.[a]	<0.01
	C	n.d.[a]	n.d.[a]	<0.01
	T	1. 6±0.2	129±15	0.12

[a] Below limits of detection.

good agreement with previous data, we found that dATP was inserted opposite dT in the template with a k_{cat}/K_M of $7.7\times10^8\,M^{-1}min^{-1}$. We then examined the insertion of d**MMO2**TP and d**DMO**TP opposite d**5SICS** under identical conditions. We found that that d**MMO2**TP and d**DMO**TP are inserted with efficiencies of 3.8×10^5 and $2.2\times10^6\,M^{-1}min^{-1}$, respectively. To determine fidelity, we measured the rate of insertion of each natural triphosphate opposite d**5SICS** in the same sequence context. We found that dATP, dGTP, and dTTP are inserted with efficiencies between 9×10^3 and $1.5\times10^5\,M^{-1}min^{-1}$, but dCTP was not in-

serted at a detectable level ($k_{cat}/K_M < 1\times10^3\,M^{-1}min^{-1}$). All of the data are in good agreement with previously reported results.[6,8] We also determined the efficiency with which Taq inserts dATP opposite dT and d**MMO2**TP opposite d**5SICS** in sequence context I and observed values of 8.2×10^7 and $9.7\times10^4\,M^{-1}min^{-1}$, respectively, also in good agreement with previously reported data.[5]

Insertion efficiencies of dMMO2TP derivatives opposite d5SICS: The insertion by Kf of each d**MMO2** triphosphate derivative opposite d**5SICS** was characterized in sequence context I (Table 1). We found that the most simple derivative, d**AMO1**TP, is inserted opposite d**5SICS** with a second order rate constant of $8.6\times10^4\,M^{-1}min^{-1}$. d**AMO3**TP was inserted with a similar efficiency ($1.1\times10^5\,M^{-1}min^{-1}$), but d**AMO2**TP was inserted sixfold less efficiently ($1.5\times10^4\,M^{-1}min^{-1}$). However, d**PMO1**TP and d**NMO1**TP were inserted with higher efficiencies of 2.0×10^6 and $2.3\times10^6\,M^{-1}min^{-1}$, respectively. The increased efficiency of d**PMO1**TP and d**NMO1**TP insertion opposite d**5SICS** by Kf resulted from both an increase in the apparent k_{cat} and a decrease in the apparent K_M.

We next characterized the ability of Taq to insert each d**MMO2**TP derivative opposite d**5SICS** in the same sequence context (Table 2). We found that Taq inserts d**DMO**TP with an efficiency of $1.6\times10^5\,M^{-1}min^{-1}$, which is virtually identical to the efficiency of d**MMO2**TP insertion. We found that Taq inserts d**AMO1**TP, d**AMO2**TP, and d**AMO3**TP opposite d**5SICS** much less efficiently, with second order rate constants of 4.9×10^3, 1.2×10^3, and $1.6\times10^3\,M^{-1}min^{-1}$, respectively. Although insertion of d**PMO1**TP opposite d**5SICS** by Taq was also not very efficient ($3.2\times10^4\,M^{-1}min^{-1}$), insertion of d**NMO1**TP was significantly more efficient ($4.3\times10^5\,M^{-1}min^{-1}$).

Of the new d**MMO2** analogues examined, the most promising in sequence context I are d**PMO1**TP, and especially d**NMO1**TP, thus, we next determined whether their insertion efficiency by Kf opposite d**5SICS** is dependent on sequence context, using sequence context II (Table 3). Again, for comparison, we redetermined the efficiencies of dATP, d**MMO2**TP or d**DMO**TP insertion opposite their cognate base in the same sequence context. The natural base pair was synthesized with an efficiency of $5.8\times10^8\,M^{-1}min^{-1}$, whereas d**MMO2**TP was inserted opposite d**5SICS** with an efficiency of $1.9\times10^5\,M^{-1}min^{-1}$; both values are in good agreement with previously reported data.[13] Kf inserts d**DMO**TP opposite d**5SICS** with an efficiency of $3.9\times10^5\,M^{-1}min^{-1}$. Interestingly, we found that insertion of both d**PMO1**TP and d**NMO1**TP opposite d**5SICS** by Kf is approximately four- and eightfold more efficient than insertion of d**DMO**TP and d**MMO2**TP, respectively.

Table 2. Kinetic data for Taq-mediated insertion of triphosphates (d**Y**TP) opposite d**5SICS** or d**NaM** in the template in sequence context I; insertion of dATP opposite dT is provided for comparison.

5′-d(TAATACGACTCACTATAGGGAGA)
3′-d(ATTATGCTGAGTGATATCCCTCT**X**GCTAGGTTACGGCAGGATCGC)

X	Y	k_{cat} [min^{-1}]	K_M [μM]	k_{cat}/K_M [$\times10^5\,M^{-1}min^{-1}$]
T	A	2.6±0.2	0.032±0.002	820
5SICS	**NaM**	2.7±0.4	0.35±0.04	76
	DMO	3.3±1.7	21.0±0.5	1.6
	MMO2	3.4±0.3	35.0±6.0	0.97
	NMO1	5.5±0.2	12.8±3.4	4.3
	PMO1	3.6±1.4	113±25	0.32
	AMO1	0.83±0.13	170±31	0.049
	AMO3	0.35±0.06	214±28	0.016
	AMO2	0.45±0.06	370±36	0.012
	5SICS	3.4±0.5	189±16	0.18
	A	0.5±0.05	147±7	0.035
	G	4.5±0.1	216±42	0.21
	C	n.d.[a]	n.d.[a]	<0.01
	T	0.8±0.1	303±19	0.026
NaM	**5SICS**	2.4±0.6	0.34±0.03	71
	NaM	7.9±1.4	151±9	0.52
	A	4.0±0.8	84.0±4.0	0.48
	G	n.d.[a]	n.d.[a]	<0.01
	C	n.d.[a]	n.d.[a]	<0.01
	T	1.0±0.2	421±71	0.024

[a] Below limits of detection.

Table 3. Kinetic data for Kf-mediated insertion of triphosphates (d**Y**TP) opposite d**5SICS** or d**NaM** in the template in sequence context II; insertion of dATP opposite dT is provided for comparison.

5′-d(TAATACGACTCACTATAGGGAGC)
3′-d(ATTATGCTGAGTGATATCCCTCG**X**TCTAGGTTACGGCAGGATCGC)

X	Y	k_{cat} [min^{-1}]	K_M [μM]	k_{cat}/K_M [$\times10^5\,M^{-1}min^{-1}$]
T	A	0.95±0.10	0.0017±0.0001	5800
5SICS	**NaM**	11.4±2.3	0.41±0.01	280
	DMO	14.2±1.1	35.8±1.5	3.9
	MMO2	8.6±0.2	46.6±7.1	1.9
	NMO1	33.6±7.0	23.0±0.1	15
	PMO1	19.0±1.6	13.5±1.5	14
NaM	**5SICS**	5.8±1.1	0.049±0.003	1200

Efficiency and fidelity of dNaM–d5SICS synthesis: To provide a reference for how efficiently and selectively Taq synthesizes d**NaM**–d**5SICS**, we first measured the efficiency of Kf-mediated synthesis of d**NaM**–d**5SICS** and all possible mispairs in both strand contexts of sequence context I (Table 1). We found that d**5SICS**TP is inserted opposite d**NaM** with an efficiency of $2.1\times10^8\,M^{-1}min^{-1}$, in good agreement with previously reported data.[13] However, we found that d**NaM**TP is inserted opposite d**5SICS** with an efficiency of $5.8\times10^7\,M^{-1}min^{-1}$. Although significantly greater than reported previously for this sequence context, it is similar to that reported for the same insertion in sequence context II.[13] To confirm the rates for insertion in sequence context II, we reanalyzed the synthesis of d**NaM**–d**5SICS** in both strand contexts of sequence context II (Table 3). We found that d**5SICS**TP is inserted opposite d**NaM** and that d**NaM**TP is inserted opposite d**5SICS** with efficiencies of 1.2×10^8 and $2.8\times10^7\,M^{-1}min^{-1}$, respectively, both in good agreement with the previously published data.

As already mentioned, the most efficiently inserted dNTP opposite d**5SICS** by Kf was dGTP, which we found to proceed with an efficiency of $1.5\times10^5\,\text{M}^{-1}\,\text{min}^{-1}$, although dATP and dTTP were inserted less efficiently, dCTP was not inserted at detectable level, and d**5SICS**TP was inserted with an efficiency of $2.9\times10^5\,\text{M}^{-1}\,\text{min}^{-1}$ (Table 1). With d**NaM** in the template, the natural triphosphate most efficiently inserted by Kf was dATP, which proceeded with an efficiency of $1.8\times10^6\,\text{M}^{-1}\,\text{min}^{-1}$ (Table 1). dTTP was also inserted, but with a reduced efficiency of $1.2\times10^4\,\text{M}^{-1}\,\text{min}^{-1}$, whereas dGTP and dCTP were not inserted at detectable levels ($k_{cat}/K_M<10^3\,\text{M}^{-1}\,\text{min}^{-1}$). d**NaM**TP was inserted opposite d**NaM** with an efficiency of $9.5\times10^6\,\text{M}^{-1}\,\text{min}^{-1}$. The rates for the synthesis of these mispairs are all in good agreement with previously published data.[13]

We next determined the efficiency and fidelity of d**NaM**–d**5SICS** synthesis by Taq in both strands of sequence context I. Again, for comparison we first measured the efficiency with which Taq inserted dATP opposite dT in the same sequence context, which we found to be $8.2\times10^7\,\text{M}^{-1}\,\text{min}^{-1}$. We found that Taq inserts d**NaM**TP opposite d**5SICS** and d**5SICS**TP opposite d**NaM** with efficiencies of 7.6×10^6 and $7.1\times10^6\,\text{M}^{-1}\,\text{min}^{-1}$, respectively. With d**5SICS** in the template, Taq inserted dGTP more efficiently than the other natural triphosphates, with an efficiency of $2.1\times10^4\,\text{M}^{-1}\,\text{min}^{-1}$, followed by dATP and dTTP, with efficiencies of 3.5×10^3 and $2.6\times10^3\,\text{M}^{-1}\,\text{min}^{-1}$, respectively. Taq did not insert dCTP at a detectable rate ($<10^3\,\text{M}^{-1}\,\text{min}^{-1}$). The most competitive mispair synthesized resulted from the insertion of d**5SICS**TP, which proceeded with an efficiency of only $1.8\times10^4\,\text{M}^{-1}\,\text{min}^{-1}$. With d**NaM** in the template, Taq inserted dATP most efficiently, with a second order rate constant of $4.8\times10^4\,\text{M}^{-1}\,\text{min}^{-1}$. dTTP was inserted with an efficiency of $2.4\times10^3\,\text{M}^{-1}\,\text{min}^{-1}$, whereas dGTP and dCTP were inserted with undetectable rates ($<10^3\,\text{M}^{-1}\,\text{min}^{-1}$). d**NaM**TP was inserted opposite d**NaM** by Taq with an efficiency of $5.2\times10^4\,\text{M}^{-1}\,\text{min}^{-1}$.

Efficiency and fidelity of PCR amplification: To begin to examine unnatural base pair replication, which includes synthesis and extension in both strand contexts, we first explored the Taq-mediated PCR amplification of DNA containing d**5SICS** paired opposite either d**NaM**, d**MMO2**, d**DMO**, d**NMO1**, or d**PMO1**. Taq was employed despite its low fidelity for replication of the unnatural base pair, because it lacks exonuclease proofreading activity, to facilitate comparison with the steady-state kinetic data. In addition, the unnatural base pairs were incorporated into the 134 nt DNA template, D6, in the middle of a six nucleotide randomized region.[9] The randomized template was selected to provide the strictest possible measure of fidelity as sequences with inherently low fidelity are expected to lose the unnatural base pair and then efficiently amplify. While it is not practical to characterize fidelity in these reactions due to the significant read through, sequencing traces clearly indicate that while d**5SICS**–d**NaM** is best replicated, amongst the other analogues, d**NMO1** is optimized for pairing opposite d**5SICS**, followed by d**DMO**, d**MMO2**, and d**PMO1** (Figure S28 in the Supporting Information).

To examine amplification under more practical and high fidelity conditions we explored PCR using the exonuclease proficient Deep Vent polymerase of the same unnatural base pairs positioned in the middle of the 149 nt duplex referred to as D1, which was used previously to characterize the amplification of d**NaM**–d**5SICS** and d**MMO2**–d**5SICS**[9] (Table 4 and Figure S29 in the Supporting Information). In this case, fidelity was characterized as described previously.[9] In agreement with previous results, d**NaM**–d**5SICS** was replicated with a remarkable fidelity of 99.7. Interestingly, d**NMO1**–d**5SICS**, d**DMO**–d**5SICS**, and d**MMO2**–d**5SICS** were also amplified with a similar fidelity, while as predicted by the steady-state kinetic data, d**PMO1**–d**5SICS** was amplified with a significantly lower fidelity.

Table 4. Fidelities of Deep Vent-mediated PCR amplification of unnatural base pairs.[a]

Base pair	Fidelity[b]
d**NaM**–d**5SICS**	99.7
d**DMO**–d**5SICS**	99.7
d**MMO2**–d**5SICS**	99.7
d**PMO1**–d**5SICS**	92.4
d**NMO1**–d**5SICS**	99.5

[a] See text for experimental details. [b] Fidelity is defined as % unnatural base pair retention per doubling; see ref. [9].

Discussion

The identification d**MMO2**–d**5SICS** was a landmark in our efforts to identify an unnatural base pair, and early efforts directed toward its optimization yielded d**DMO**–d**5SICS** and in particular d**NaM**–d**5SICS**. While the former was slightly better replicated than d**MMO2**–d**5SICS**, d**NaM**–d**5SICS** was replicated significantly better, although whether this was unique to Kf, or a general property of the unnatural base pair was not known. In addition, the strategy of using nucleobases with little or no structural homology to their natural counterparts makes possible many different substituents, and it is unclear whether d**NaM**–d**5SICS** represents the best route to optimize d**MMO2**–d**5SICS**, especially considering the increased potential for linker modification of the more simple scaffolds.

In an effort to optimize the d**MMO2** scaffold for pairing with d**5SICS**, we examined derivatives with different substituents in place of the *para* methyl group. Specifically, five different substituents expected to alter the physicochemical properties of the nucleobases were examined, including amine, amide, trifluoroamide, nitro, and pyrrolo groups. The amine substituent is electron donating and expected to introduce a dipole along the C–N bond directed toward the aromatic ring. The amine group is also expected to form H bonds with water molecules. While the amide groups are

less electron donating, along with increased steric demands, they introduce increased H bonding relative to the amine. The pyrrolo substituent reduces the electron donating ability of the nitrogen and adds steric bulk, but within the context of decreased H bonding and increased stacking potential. In contrast, the nitro group is electron withdrawing and expected to introduce a significant dipole oriented along the carbon–nitrogen bond away from the aromatic ring. However, like the pyrrolo substituent, the nitro group is expected to decrease H bonding, being only a moderate H bond acceptor, and increase the ability of the nucleobase analogue to stack with flanking nucleobases within the developing duplex.

With both Kf and Taq, the analogues examined clearly separate into two groups: d**AMO1**TP, d**AMO2**TP, and d**AMO3**TP are inserted less efficiently opposite d**5SICS** than d**MMO2**TP; and d**NMO1**TP and d**PMO1**TP are inserted more efficiently. For d**AMO1**TP, the decrease is fourfold with Kf, while with Taq it was 20-fold, with the difference between the polymerases largely due to changes in the apparent k_{cat}; the modification increases k_{cat} with Kf and decreases it with Taq while the K_M was similarly increased (~fivefold) with both enzymes. Because, the amino group is expected to increase the electron density of the nucleobase ring, the observed decrease in insertion efficiencies suggests that any favorable increase in packing due to increased polarizability is offset by other deleterious factors, such as forced desolvation of the amino group, which is consistent with a similar effect on K_M observed with both enzymes. Modification of the amine with the acetyl group of d**AMO2**TP decreases insertion efficiency by both enzymes, relative to d**MMO2**TP, by a factor of 26 with Kf and more than a factor of 83 with Taq. The large reduction in efficiency with Taq results from a significant decrease in apparent binding, and an even larger decrease in turnover. Modification of the amino group with the trifluoroacetyl group of d**AMO3**TP also reduced the efficiency of insertion, but very differently with the two enzymes. With Kf, the decrease is only fourfold relative to d**MMO2**TP, but it is more than 60-fold with Taq. The large decrease in recognition by Taq again results from both reduced binding and reduced turnover. Thus, insertion of these analogues appears to be limited by desolvation and steric or electrostatic clashes that are polymerase specific and generally more severe with Taq.

Relative to d**MMO2**TP, the behavior of d**PMO1**TP and d**NMO1**TP are very different from that of the other analogues with both Kf and Taq. With Kf, in both sequence contexts I and II, d**PMO1**TP and d**NMO1**TP are each inserted approximately fivefold more efficiently, due to increased binding and increased turnover. In contrast, with in sequence context I, d**PMO1**TP is inserted by Taq threefold less efficiently then d**MMO2**TP, due to reduced binding, but d**NMO1**TP is inserted fourfold more efficiently, due to a small increase in turnover and a slightly larger increase in apparent binding affinity. The data suggest that with Kf the presence of the nitro or the pyrrole group likely reduces the cost of desolvation relative to the amine or amide and also mediates favorable packing interactions with d**5SICS** or the polymerase in the developing transition state. As with the other analogues, Taq appears to be less accommodating to alterations in the size of the substituent and tolerates the nitro substituent, but not the pyrrole group.

The detailed kinetic analysis focused on the insertion of the different triphosphate analogue opposite d**5SICS**. However, replication requires base pair synthesis in the other strand context, the insertion of d**5SICS**TP opposite the analogue in template DNA, as well as the continued primer elongation in both strand contexts. The results of the PCR analysis suggest that the nitro and pyrrolo substituents of d**NMO1** and d**PMO1**, respectively, do not significantly interfere with any of these other steps of replication. Moreover, the fidelities observed during PCR with Taq indicate that the improvement in steady-state triphosphate insertion characterized for d**NMO1**TP is also manifest as improved replication.

Generally, the data obtained with the five new analogues examined suggest that optimizing hydrophobicity, including reducing the cost of desolvation, and improving packing in the developing major groove are the most efficacious routes to optimization of the d**MMO2** scaffold, although the interactions must be more carefully manipulated with Taq than with Kf, apparently due to a more discriminating active site. The importance of hydrophobicity and packing is also consistent with the remarkable insertion efficiency of d**NaM** opposite d**5SICS**. If supported by further study, these arguments suggest that, at least from the perspective of the *para* position of the d**MMO2** scaffold, the developing major groove of the duplex within the polymerase active site is able to accommodate planar aromatic groups with favorable packing interactions, but the waters and metal ions found within the major groove of free duplex DNA are not yet available. Regardless of the underlying mechanism, the steady-state kinetic and PCR data indicate that d**NMO1** is the most promising d**MMO2** analogue yet identified.

Previous data collected for the Kf-mediated synthesis of d**NaM**–d**5SICS** suggested that its efficiency is strand and sequence context specific. However, this was based on the efficiency of a single step in a single sequence context, the insertion of d**NaM**TP opposite d**5SICS** in sequence context I, which appeared to be significantly less efficient than that in sequence context II, or than the insertion of d**5SICS**TP opposite d**NaM** in either sequence context. The efficiency of this reaction was re-evaluated in the current work and we found that the previous data underestimated the rate approximately tenfold, which we attribute to the presence of an impurity. The corrected data places the efficiency of d**NaM**TP insertion on par with that of the others. Thus, the replication of d**NaM**–d**5SICS** does not appear to be either strongly strand or sequence context dependent. The efficiency of both steps of unnatural base pair synthesis are within four- to 13-fold that of a natural base pair. Moreover, relative to the most competitive mispair, the overall fidelity when both unnatural base pair synthesis and extension[13] are combined is at least 10^4. To our knowledge, this repre-

sents the most efficient and high fidelity replication reported to date for an unnatural base pair.

The synthesis of d**NaM**–d**5SICS** by Kf is remarkably efficient and selective, and it appears to be just as efficiently synthesized by Taq. Taq inserts both d**NaM**TP opposite d**5SICS** and d**5SICS**TP opposite d**NaM** only tenfold less efficiently than a natural base pair in the same sequence context. Moreover, none of the natural dNTPs was inserted efficiently opposite either d**5SICS** or d**NaM** in the template, resulting in 150-fold or greater fidelities for this step alone. The efficient and selective recognition of d**NaM**–d**5SICS** by both Kf and Taq now allow us to conclude that the determinants of efficient replication are inherent to the nucleotides themselves.

Conclusion

The data reveal that reducing the cost of nucleotide desolvation and optimizing packing interactions within the developing major groove are promising routes to optimize the efficiency of polymerase-mediated insertion of the d**MMO2**TP analogues opposite d**5SICS**, and that other than d**NaM**, d**NMO1** is the most promising analogue identified to date. While continued efforts toward the optimization of the d**NMO1** scaffold are justified by its potential for accommodating linkers, the data reported herein for d**NaM**–d**5SICS** demonstrate just how challenging the identification of a more optimized base pair is likely to be. Thus, the data strongly suggest that efforts toward developing an unnatural base pair for in vitro applications should focus on the d**NaM** scaffold, including efforts to identify suitable sites for linker attachment to facilitate applications based on the site-specific modification of DNA or RNA. Such efforts are currently underway.

Experimental Section

General: All reactions were carried out in oven-dried glassware under inert atmosphere, and all solvents were dried over 4 Å molecular sieves with the exception of tetrahydrofuran, which was distilled from sodium metal. All other reagents were purchased from Fisher or Aldrich. ^{1}H, ^{13}C and ^{31}P NMR spectra were recorded on Bruker DRX-600, DRX-500 or Varian Inova-300 spectrometers. High-resolution mass spectroscopic data were obtained on an ESI-ToF mass spectrometer (Agilent 6200 Series) at the TSRI Open Access Mass Spectrometry Laboratory, and MALDI-ToF mass spectrometry (Applied Biosystems Voyager DE-PRO System 6008) was from the TSRI Center for Protein and Nucleic Acid Research.

Synthesis procedures and characterizations

Compound 1: This was synthesized according to the literature.[29]

Compound 2: $NaHCO_3$ (1.65 g, 19.4 mmol, 1.2 equiv) was added to a solution of *m*-anisidine (2 mL, 16.2 mmol, 1 equiv) in tetrahydrofuran (50 mL) at 0 °C. Benzyl chloroformate (2.8 mL, 19.4 mmol, 1.2 equiv) was then added dropwise under strong stirring. The mixture was allowed to warm to room temperature over 20 min, stirred for an additional hour and then diluted with CH_2Cl_2. The organic layer was quenched with saturated aqueous $NaHCO_3$, washed with brine, dried (Na_2SO_4), filtered and evaporated. The residue was subjected to a short silica gel column chromatography with a step gradient of CH_2Cl_2 (20–100 %) in hexane affording pure NH-Cbz *m*-anisidine. Silver nitrate (4.48 g, 14.37 mmol) and iodine (3.65 g, 14.37 mmol) were added to a solution of the Cbz-protected *m*-anisidine in MeOH (120 mL) at −20 °C. The mixture was stirred at −20 °C for 1 h, quenched by saturated aqueous $Na_2S_2O_3$ (80 mL) and filtered through a Celite pad. The filtrate was concentrated to 10 % of its original volume and diluted with CH_2Cl_2 (200 mL). The organic layer was quenched with saturated aqueous $NaHCO_3$, washed with brine, dried (Na_2SO_4), filtered and evaporated. The residue was subjected to silica gel column chromatography with a step gradient of CH_2Cl_2 (20–80 %) in hexane. The desired compound **2** was obtained as white foam after evaporation of the solvent (4.04 g, 10.54 mmol, 65 % yield). ^{1}H NMR (400 MHz, [D$_6$]DMSO): δ = 9.89 (s, 1H, NH), 7.60 (d, J = 8.5 Hz, 1H), 7.40 (m, 5H), 7.27 (d, J = 2.3 Hz, 1H), 6.90 (m, 1H), 5.16 (s, 2H), 3.76 ppm (s, 3H); ^{13}C NMR (100 MHz, $CDCl_3$): δ = 158.66, 153.08, 139.53, 139.13, 135.79, 128.67, 128.49, 128.31, 112.37, 102.07, 78.04, 67.22, 56.33 ppm; HRMS (ESI$^+$) m/z: calcd for $C_{15}H_{15}INO_3$ $[M+H]^+$ 384.0091, found 384.0097.

Compound 3: A mixture of palladium acetate (880 mg, 3.92 mmol, 0.15 equiv) and triphenylarsine (2 g, 3.92, 0.15 equiv) in dry dimethylformamide (150 mL) was stirred under argon atmosphere at room temperature for 20 min. Compound **2** (15 g, 39.2 mmol, 1.5 equiv), **1** (9 g, 26.1 mmol, 1 equiv) and tri-*n*-butylamine (9.3 mL, 39.2 mmol, 1.5 equiv) in dimethylformamide (5 mL) were added to this mixture, and the resulting reaction mixture was stirred under nitrogen at 70 °C for 15 h. The mixture was cooled to 0 °C and tetrabutylammonium fluoride (1 M; 44 mL, 44 mmol) in tetrahydrofuran was added, and the mixture was stirred for 2 h while being warmed to room temperature. The reaction mixture was filtered through Celite and extracted with ethyl acetate and saturated aqueous $NaHCO_3$. The combined organic layers were dried (Na_2SO_4), filtered and evaporated. The residue was subjected to silica gel column chromatography with a step gradient of ethyl acetate (5–30 %) in CH_2Cl_2. The eluted product was dissolved in acetic acid (50 mL) and acetonitrile (50 mL). The solution was cooled to 0 °C, sodium triacetoxyborohydride (4.5 g, 21.23 mmol) was added, and the mixture was stirred for 1 h. The reaction mixture was diluted with ethyl acetate, quenched with saturated aqueous $NaHCO_3$, washed with brine, dried (Na_2SO_4), filtered and evaporated. The residue was subjected to silica gel column chromatography with a step gradient of methanol (0–4 %) in ethyl acetate. The desired compound **3** was obtained as white foam after evaporation of the solvent (6.58 g, 17.62 mmol, 45 % yield). ^{1}H NMR (400 MHz, MeOD): δ = 7.49–7.27 (m, 6H, H-ar, H-6), 7.26–7.17 (m, 1H, H-3), 6.95 (dd, J = 8.2, 2.0 Hz, 1H, H-5), 5.39 (dd, J = 10.2, 5.5 Hz, 1H, H-1′), 5.17 (s, 2H, OCH_2Ar (Cbz)), 4.35–4.24 (m, 1H, H-3′), 3.93 (td, J = 5.2, 2.7 Hz, 1H, H-4′), 3.81 (s, 3H, OCH_3), 3.74–3.59 (m, 2H, H-5′,H-5″), 2.27 (ddd, J = 13.1, 5.6, 1.9 Hz, 1H, H-2′), 1.82 ppm (ddd, J = 13.1, 10.3, 6.1 Hz, 1H, H-2″); ^{13}C NMR (100 MHz, MeOD): δ = 156.7 ($C_{2(C-OMe)}$), 154.4 (NHC=O), 139.1 ($C_{4(C-NHCbz)}$), 136.6 (Cq, Car), 128.1–127.6 (CH, Ar), 126.0 (C_6), 124.6 ($C_{1(C-sugar)}$), 110.2 (C_5), 101.2 (C_3), 87.1 ($C_{4'}$), 74.8 ($C_{1'}$), 73.0 ($C_{3'}$), 66.1 (OCH_2Ph), 62.7 ($C_{5'}$), 54.3 (OCH_3), 41.7 ($C_{2'}$); HRMS (ESI$^+$) m/z: calcd for $C_{20}H_{24}NO_6$ $[M+H]^+$ 374.1598, found 374.1615.

Compound 4: 1,3-Dichloro-1,1,3,3-tetraisopropyldisiloxane (2.6 mL, 8.1 mmol, 1.2 equiv) was added to a solution of **3** (2.5 g, 6.7 mmol, 1 equiv) in dry pyridine (100 mL), dropwise over 15 min. The reaction mixture was stirred for 2 h at room temperature under nitrogen atmosphere, concentrated twofold and diluted with CH_2Cl_2. The organic layer was quenched with saturated aqueous $NaHCO_3$, washed with brine, dried (Na_2SO_4), filtered and evaporated. The residue was dissolved in ethyl acetate (75 mL) and Et_3N (250 μL, 1.76 mmol) was added. The resulting solution was treated with 10 % Pd/C (150 mg) under H_2 atmosphere and allowed to stir until the presence of the starting material could no longer be detected by TLC (~1 h). The reaction mixture was filtered through Celite and the filtrate was extracted with ethyl acetate and saturated aqueous $NaHCO_3$. The combined organic layers were dried (Na_2SO_4), filtered and evaporated. The residue was subjected to a silica gel column chromatography with a step gradient with ethyl acetate (0–5 %) in CH_2Cl_2 containing 0.5 % triethylamine. The desired compound **4** was obtained as a colorless oil after evaporation of the solvent (21 g, 4.28 mmol, 64 % yield). ^{1}H NMR (500 MHz, CD_3CN): δ = 7.10 (d, J = 8.1 Hz, 1H, H-6), 6.26 (d, J = 2.1 Hz, 1H, H-3), 6.18 (dd, J = 8.1, 2.1 Hz, 1H, H-5), 5.15

(m, 1H, H-1′), 4.47 (dt, J=7.7, 5.6 Hz, 1H, H-3′), 4.11 (s, 2H, NH_2), 4.05–3.84 (m, 2H, H-5′,H-5″), 3.75–3.68 (m, 4H, OCH_3, H-4′), 2.20 (ddd, J=12.7, 7.3, 5.4 Hz, 1H, H-2′), 2.00 (m, 1H, H-2″), 1.13–1.00 ppm (m, 28H, *i*Pr); ^{13}C NMR (125 MHz, CD_3CN): δ=158.3 (C_2), 149.6 (C_4), 128.0 (C_6), 120.2 (C_1), 107.1 (C_5), 98.6 (C_3), 86.3 ($C_{4'}$), 74.3 ($C_{1'}$), 74.0 ($C_{3'}$), 64.2 ($C_{5'}$), 55.8 (OCH_3), 42.5 ($C_{2'}$), 17.9–13.4 ppm (*i*Pr); HRMS (ESI$^+$) m/z: calcd for $C_{24}H_{44}NO_5Si_2$ $[M+H]^+$ 482.2752, found 482.2748.

Compound 5a: A solution of 70% aqueous *tert*-butyl hydroperoxide (160 μL, 1.18 mmol, 3.8 equiv) was added dropwise over a period of 15 min to a solution of **4** (150 mg, 0.31 mmol, 1 equiv) and potassium iodide (5.1 mg, 0.031 mmol, 0.1 equiv) in CH_3CN (1.1 mL), and the mixture was stirred at 75°C in the dark for 2 h. The mixture was quenched with saturated aqueous $Na_2S_2O_3$, washed with brine, extracted with ethyl acetate, dried (Na_2SO_4), filtered and evaporated. The resulting residue was dissolved in tetrahydrofuran (1.5 mL), tetrabutylammonium fluoride (1 M; 0.5 mL, 0.5 mmol) in tetrahydrofuran was added, and the mixture was stirred for 1 h at room temperature. The reaction mixture was diluted with ethyl acetate, quenched with saturated aqueous $NaHCO_3$, washed with brine, dried (Na_2SO_4), filtered and evaporated. The residue was subjected to silica gel column chromatography with a step gradient of methanol (0–4%) in ethyl acetate. The desired compound **5a** was obtained as white foam after evaporation of the solvent (32 mg, 0.12 mmol, 38%). ^{1}H NMR (500 MHz, CD_3CN): δ=7.82 (dd, J=8.4, 2.2 Hz, 1H, H-5), 7.77–7.69 (m, 2H, H-6, H-3), 5.32 (dd, J=10.1, 5.8 Hz, 1H, H-1′), 4.24 (dt, J=5.2, 2.1 Hz, 1H, H-3′), 3.91 (s, 3H, OCH_3), 3.88 (td, J=5.0, 2.6 Hz, 1H, H-4′), 3.63–3.59 (dd, J=5.0, 0.9 Hz, 2H, H-5′, H-5″), 2.32 (ddd, J=13.0, 5.7, 2.0 Hz, 1H), 1.68 ppm (ddd, J=13.1, 10.1, 5.9 Hz, 1H); ^{13}C NMR (125 MHz, CD_3CN): δ=157.4 (C_2), 149.0 (C_4), 140.3 (C_1), 127.1 (C_6), 116.6 (C_5), 106.1 (C_3), 88.5 ($C_{4'}$), 75.5 ($C_{1'}$), 73.9 ($C_{3'}$), 63.7 ($C_{5'}$), 56.8 (OCH_3), 42.9 ppm ($C_{2'}$); HRMS (ESI$^+$) m/z: calcd for $C_{12}H_{16}NO_6$ $[M+H]^+$ 270.0972, found 270.0984.

Compound 5b: A solution of **4** (250 mg, 0.52 mmol, 1 equiv) and 2,5-dimethoxytetrahydrofuran (170 mg, 1.3 mmol, 2.5 equiv) in H_2O (0.8 mL) was heated to 140°C for 30 min in a microwave synthesizer (Biotage AB, Sweden). The reaction was allowed to cool and the resulting mixture was diluted with ethyl acetate, quenched with saturated aqueous $NaHCO_3$, washed with brine, dried (Na_2SO_4), filtered and evaporated. The resulting residue was dissolved in tetrahydrofuran (3 mL), tetrabutylammonium fluoride (1 M; 1 mL, 1 mmol) in tetrahydrofuran was added and the mixture was stirred for 1 h at room temperature. The reaction mixture was diluted with ethyl acetate, quenched with saturated aqueous $NaHCO_3$, washed with brine, dried (Na_2SO_4), filtered and evaporated. The residue was subjected to silica gel column chromatography with a step gradient of methanol (0–8%) in CH_2Cl_2. The desired compound **5b** was obtained as white foam after evaporation of the solvent (95 mg, 0.33 mmol, 63%). ^{1}H NMR (600 MHz, CD_3CN): δ=7.52 (d, J=8.0 Hz, 1H, H-6), 7.17 (m, J=2.1 Hz, 2H, H-7), 7.02 (m, 2H, H-5, H-3), 6.29 (t, J=2.2 Hz, 2H, H-8), 5.30 (dd, J=10.2, 5.6 Hz, 1H, H-1′), 4.23 (m, 1H, H-3′), 3.88 (s, 2H, OCH_3), 3.83 (td, J=5.0, 2.6 Hz, 1H, H-4′), 3.60 (t, J=5.1 Hz, 2H), 3.21 (d, J=3.7 Hz, 1H, OH-3′), 2.92 (t, J=5.7 Hz, 1H, OH-5′), 2.22 (m, 1H, H-2′), 1.76 ppm (ddd, J=13.0, 10.3, 6.0 Hz, 1H, H-2″); ^{13}C NMR (150 MHz, CD_3CN): δ=158.1 (C_2), 141.6 (C_4), 129.1 (C_6), 128.0 (C_1), 120.2 (C_7), 112.6 (C_5), 111.1 (C_8), 104.0 (C_3), 88.2 ($C_{4'}$), 75.4 ($C_{1'}$), 74.1 ($C_{3'}$), 63.8 ($C_{5'}$), 56.4 (OCH_3), 43.1 ppm ($C_{2'}$); HRMS (ESI$^+$) m/z: calcd for $C_{16}H_{20}NO_4$ $[M+H]^+$ 290.1387, found 290.1397.

Compound 5c: Triethylamine (125 μL, 0.89 mmol, 1.7 equiv) and then acetic anhydride (60 μL, 0.62 mmol, 1.2 equiv) were added dropwise to a solution of **4** (250 mg, 0.52 mmol, 1 equiv) in CH_2Cl_2 (600 μL). The reaction mixture was stirred at room temperature for 20 min and then quenched with saturated aqueous $NaHCO_3$. The organic layer was diluted with CH_2Cl_2, washed with brine, dried (Na_2SO_4), filtered and evaporated. The resulting residue was dissolved in tetrahydrofuran (2 mL), tetrabutylammonium fluoride (1 M; 1 mL, 1 mmol) in tetrahydrofuran was added and the mixture was stirred for 1 h at room temperature. The reaction mixture was diluted with ethyl acetate, quenched with saturated aqueous $NaHCO_3$, washed with brine, dried (Na_2SO_4), filtered and evaporated. The residue was subjected to silica gel column chromatography with a step gradient of methanol (0–12%) in CH_2Cl_2. The desired compound **5c** was obtained as white foam after evaporation of the solvent (75 mg, 0.27 mmol, 51% yield). ^{1}H NMR (600 MHz, CD_3OD): δ=7.40 (d, J=8.3 Hz, 1H, H-6), 7.33 (d, J=1.8 Hz, 1H, H-3), 7.02 (dd, J=8.3, 1.8 Hz, 1H, H-5), 5.38 (dd, J=10.2, 5.6 Hz, 1H, H-1′), 4.27 (m, 1H, H-3′), 3.90 (td, J=5.2, 2.7 Hz, 1H, H-4′), 3.80 (s, 3H, OCH_3), 3.65 (m, 2H, H-5′, H-5″), 2.27 (ddd, J=13.1, 5.5, 1.7 Hz, 1H, H-2′), 2.10 (s, 3H, $COCH_3$), 1.80 ppm (ddd, J=13.2, 10.3, 6.0 Hz, 1H, H-2″); ^{13}C NMR (150 MHz, CD_3OD): δ=171.5 (NHC=O), 157.8 (C_2), 140.1 (C_4), 127.2 (C_6), 127.2 (C_1), 112.7 (C_5), 103.7 (C_3), 88.5 ($C_{4'}$), 76.2 ($C_{1'}$), 74.4 ($C_{3'}$), 64.0 ($C_{5'}$), 55.7 (OCH_3), 43.1 ($C_{2'}$), 23.9 ppm ($COCH_3$); HRMS (ESI$^+$) m/z: calcd for $C_{14}H_{20}NO_5$ $[M+H]^+$ 282.1341, found 290.1351.

Compound 5d: Triethylamine (170 μL, 1.24 mmol, 1.7 equiv) and then trifluoroacetic anhydride (170 μL, 0.88 mmol, 1.2 equiv) were added dropwise to a solution of **4** (350 mg, 0.73 mmol, 1 equiv) in CH_2Cl_2 (2 mL) at 10°C. The reaction mixture was stirred at room temperature for 20 min at 10°C and then quenched with saturated aqueous $NaHCO_3$. The organic layer was diluted with CH_2Cl_2, washed with brine, dried (Na_2SO_4), filtered and evaporated. The resulting residue was dissolved in tetrahydrofuran (5 mL), tetrabutylammonium fluoride (1 M; 1.9 mL, 1.9 mmol) in tetrahydrofuran was added and the mixture was stirred for 1 h at room temperature. The reaction mixture was diluted with ethyl acetate, quenched with saturated aqueous $NaHCO_3$, washed with brine, dried (Na_2SO_4), filtered and evaporated. The residue was subjected to silica gel column chromatography with a step gradient of methanol (0–10%) in CH_2Cl_2. The desired compound **5c** was obtained as white foam after evaporation of the solvent (200 mg, 0.60 mmol, 81% yield). ^{1}H NMR (600 MHz, CD_3CN): δ=9.25 (s, 1H, NH), 7.50 (d, J=8.2 Hz, 1H, H-6), 7.27 (d, J=1.9 Hz, 1H, H-3), 7.19 (m, 1H, H-5), 5.27 (dd, J=10.2, 5.6 Hz, 1H, H-1′), 4.22 (m, 1H, H-3′), 3.82 (d, J=27.6 Hz, 4H, H-4′, OCH_3), 3.59 (d, J=4.9 Hz, 2H, H-5′, H-5″), 2.22 (m, 1H, H-2′), 1.72 ppm (m, 1H, H-2″); ^{13}C NMR (150 MHz, CD_3CN): δ=157.5 (C_2), 156.2–155.4 (NHC=O), 136.9 (C_4), 129.7 (C_6), 127.3 (C_1), 119.8–114.1 (CF_3), 113.7 (C_5), 104.7 (C_3), 88.2 ($C_{4'}$), 75.4 ($C_{1'}$), 74.1 ($C_{3'}$), 63.9 ($C_{5'}$), 56.2 (OCH_3), 43.1 ppm ($C_{2'}$); HRMS (ESI$^+$) m/z: calcd for $C_{14}H_{17}F_3NO_5$ $[M+H]^+$ 336.1053, found 336.1066.

General procedure for triphosphate synthesis: Proton sponge (1.3 equiv) and the free nucleoside derivative (1.0 equiv) were dissolved in dry trimethyl phosphate (40 equiv) and cooled to −15°C under nitrogen atmosphere. Freshly distilled $POCl_3$ (1.3 equiv) was added dropwise and the resulting mixture was stirred at −10°C for 2 h. Tributylamine (6.0 equiv) and a solution of tributylammonium pyrophosphate (5.0 equiv) in dimethylformamide (0.5 M) were added. Over 30 min, the reaction was allowed to warm slowly to 0°C and then was quenched by addition of 0.5 M aqueous $Et_3NH_2CO_3$ (TEAB) pH 7.5 (2 vol. equiv). The mixture was diluted twofold with H_2O and the product was isolated on a DEAE Sephadex column (GE Healthcare) with an elution gradient of 0 to 1.2 M TEAB, evaporated, co-distilled with H_2O (3×). Additional purification by reverse-phase (C18) HPLC (0–35% CH_3CN in 0.1 M TEAB, pH 7.5) was performed.

Compound 6a: ^{31}P NMR (162 MHz, D_2O): δ=−10.52 (d, J=19.8 Hz, γ-P), −10.84 (d, J=20.2 Hz, α-P), −22.92 ppm (t, J=20.1 Hz, β-P); MS (MALDI-ToF$^-$, matrix: 9-aminoacridine) m/z: $[M-H]^-$ calcd for $C_{12}H_{17}NO_{15}P_3$, 508.2; found, 508.3; $\varepsilon_{(\lambda=330\,nm)}$=2200 $M^{-1}cm^{-1}$; $\varepsilon_{(\lambda=285\,nm)}$=4800 $M^{-1}cm^{-1}$.

Compound 6b: ^{31}P NMR (162 MHz, D_2O): δ=−10.22 (d, J=19.8 Hz, γ-P), −10.75 (d, J=20.1 Hz, α-P), −22.82 ppm (t, J=20.0 Hz, β-P); MS (MALDI-ToF, matrix: 9-aminoacridine) m/z: $[M-H]^-$ calcd for $C_{16}H_{21}NO_{13}P_3$, 528.3; found 527.8; $\varepsilon_{(\lambda=283\,nm)}$=5080 $M^{-1}cm^{-1}$; $\varepsilon_{(\lambda=256\,nm)}$=10850 $M^{-1}cm^{-1}$.

Compound 6c: ^{31}P NMR (202 MHz, D_2O): δ=−6.35 (d, J=16.9 Hz, γ-P), −10.74 (d, J=19.7 Hz, α-P), −22.38 ppm (m, β-P); MS (MALDI-ToF$^-$, matrix: 9-aminoacridine) m/z: $[M-H]^-$ calcd for $C_{14}H_{21}NO_{14}P_3$, 520.2; found 519.3; $\varepsilon_{(\lambda=282\,nm)}$=2700 $M^{-1}cm^{-1}$; $\varepsilon_{(\lambda=248\,nm)}$=7500 $M^{-1}cm^{-1}$.

Compound 6d: ^{31}P NMR (162 MHz, D_2O): δ=−10.38 (d, J=19.8 Hz, γ-P), −10.87 (d, J=20.2 Hz, α-P), −22.82 ppm (t, J=20.0 Hz, β-P); MS (MALDI-ToF$^-$, matrix: 9-aminoacridine) m/z: $[M-H]^-$ calcd for $C_{14}H_{18}F_3NO_{14}P_3$, 574.2; found 573.9; $\varepsilon_{(\lambda=285\,nm)}$=3780 $M^{-1}cm^{-1}$; $\varepsilon_{(\lambda=251\,nm)}$=7450 $M^{-1}cm^{-1}$.

Compound 6e: A solution of **6d** in aqueous ammonia (28% NH_3 w/v; 1 mL) was stirred for 1 h. Ammonia was removed by vacuum concentration (SpeedVac, 20 min) and the resulting solution was separated by reverse-phase (C18) HPLC (0–35% CH_3CN in 0.1 M TEAB, pH 7.5) to provide pure compound **6e**. ^{31}P NMR (162 MHz, D_2O): $\delta = -9.21$ (d, $J = 20.0$ Hz, γ-P), −10.85 (d, $J = 20.4$ Hz, α-P), −22.62 ppm (t, $J = 20.6$ Hz, β-P); MS (MALDI-ToF, matrix: 9-aminoacridine) m/z: $[M-H]^-$ calcd for $C_{12}H_{19}NO_{13}P_3$, 478.2; found 477.8; $\varepsilon_{(\lambda = 284\ nm)} = 2450\ M^{-1}cm^{-1}$; $\varepsilon_{(\lambda = 240\ nm)} = 9250\ M^{-1}cm^{-1}$.

dNaMTP: d**NaM**TP was synthesized by using the general procedure described above, starting from d**NaM** nucleoside (Berry & Associates, Inc.). ^{31}P NMR (162 MHz, D_2O): $\delta = -8.96$ (d, $J = 19.4$ Hz, γ-P), −10.81 (d, $J = 20.1$ Hz, α-P), −22.66 ppm (t, $J = 20.2$ Hz, β-P); MS (MALDI-ToF$^-$, matrix: 9-aminoacridine) m/z: $[M-H]^-$ calcd for $C_{16}H_{20}O_{13}P_3$, 513.2; found 513.4; $\varepsilon_{(\lambda = 230\ nm)} = 75\,000\ M^{-1}cm^{-1}$.

d5SICSTP: d**5SICS**TP was synthesized by using the general procedure described above, starting from the d**5SICS** nucleoside (Berry & Associates, Inc.). ^{31}P NMR (162 MHz, D_2O): $\delta = -10.11$ (d, $J = 20.0$ Hz, γ-P), −11.05 (d, $J = 20.2$ Hz, α-P), −22.75 ppm (t, $J = 20.0$ Hz, β-P); MS (MALDI-ToF$^-$, matrix: 9-aminoacridine) m/z: $[M-H]^-$ calcd for $C_{15}H_{19}NO_{12}P_3S$, 530.3; found 529.3; $\varepsilon_{(\lambda = 365\ nm)} = 3950\ M^{-1}cm^{-1}$.

Gel-based kinetic assays: Primer oligonucleotides (Integrated DNA Technologies) were 5′-radiolabeled with T4 polynucleotide kinase (New England Biolabs) and [γ-^{32}P]-ATP (GE Biosciences) and annealed to template oligonucleotides[13] by heating to 95 °C followed by slow cooling to room temperature. Reactions were initiated by adding a solution of 2× dNTP (5 μL) to a mixture containing polymerase (0.10–1.23 nM) and primer template (40 nM) in reaction buffer (5 μL); Klenow reaction buffer (50 mM Tris-HCl, pH 7.5, 10 mM DTT, 50 μg mL^{-1} acetylated BSA) for Kf polymerase, ThermoPol reaction buffer (20 mM Tris-HCl, 10 mM $(NH_4)_2SO_4$, 10 mM KCl, 2 mM $MgSO_4$, 0.1% Triton X-100, pH 8.8) for Taq polymerase. After incubation at 25 °C (Kf) or 50 °C (Taq) for 3–10 min the reactions were quenched with loading dye (20 μL; 95% formamide, 20 mM EDTA, and sufficient amounts of bromophenol blue and xylene cyanole). Reaction products were resolved by polyacrylamide (15%) gel electrophoresis, and gel band intensities corresponding to the extended and unextended primers were quantified by phosphorimaging (Storm Imager, Molecular Dynamics) and Quantity One (BioRad) software. Plots of k_{obs} versus triphosphate concentration were fit to the Michaelis–Menten equation by using the program Origin (Microcal Software) to determine V_{max} and K_M. The k_{cat} was determined from V_{max} by normalizing by the total enzyme concentration. Each reaction was run in triplicate and standard deviations for both kinetic parameters were determined (Tables 1–3). An example of the raw kinetic data is shown in Figure S27 in the Supporting Information.

PCR amplification: DNA templates D1 and D6 were synthesized as described previously.[9] PCR amplification (see the Supporting Information for details and sequences) was carried out starting with D6 (0.1 ng) or of D1 (1 ng; Taq or DeepVent, respectively) in 1×ThermoPol reaction buffer with the following modifications: $MgSO_4$ adjusted to 6.0 mM, 0.6 or 0.7 mM of each natural dNTP (Taq or DeepVent, respectively), each unnatural triphosphate (0.1 mM), each primer (1 μM; see the Supporting Information for sequences), and Taq (0.03 unit μL^{-1}) or DeepVent (*exo*$^+$; 0.02 unit μL^{-1}) in an iCycler Thermal Cycler (Bio-Rad) under following thermal cycling conditions: 94 °C, 30 s; 48 °C, 30 s; 65 °C, 4 min, 18 or 13 cycles (Taq or DeepVent, respectively). Upon completion, PCR products were purified utilizing the PureLink™ PCR purification kit (Invitrogen), quantified by fluorescent dye binding (Quant-iT dsDNA HS Assay kit, Invitrogen) and sequenced on 3730 DNA Analyzer (Applied Biosystems) to determine fidelity of unnatural base pair replication (see the Supporting Information and ref. [9] for details).

Acknowledgements

Funding for this work was provided by the National Institute for Health (GM060005). We wish to thank Dr. Phillip Ordoukhanian, director of The Center for Protein and Nucleic Acids Research at The Scripps Research Institute, for analytical support.

[1] J. Horlacher, M. Hottiger, V. N. Podust, U. Hübscher, S. A. Benner, *Proc. Natl. Acad. Sci. USA* **1995**, *92*, 6329–6333.
[2] M. J. Lutz, H. A. Held, M. Hottiger, U. Hübscher, S. A. Benner, *Nucleic Acids Res.* **1996**, *24*, 1308–1313.
[3] J. A. Piccirilli, T. Krauch, S. E. Moroney, S. A. Benner, *Nature* **1990**, *343*, 33–37.
[4] Z. Yang, F. Chen, S. G. Chamberlin, S. A. Benner, *Angew. Chem.* **2010**, *122*, 181–184; *Angew. Chem. Int. Ed.* **2010**, *49*, 177–180.
[5] G. T. Hwang, F. E. Romesberg, *J. Am. Chem. Soc.* **2008**, *130*, 14872–14882.
[6] A. M. Leconte, G. T. Hwang, S. Matsuda, P. Capek, Y. Hari, F. E. Romesberg, *J. Am. Chem. Soc.* **2008**, *130*, 2336–2343.
[7] A. M. Leconte, F. E. Romesberg, in *Protein Engineering* (Ed.: C. K. a. U. L. RajBhandary), Springer, Berlin, **2009**, pp. 291–314.
[8] D. A. Malyshev, D. A. Pfaff, S. I. Ippoliti, G. T. Hwang, T. J. Dwyer, F. E. Romesberg, *Chem. Eur. J.* **2010**, *16*, 12650–12659.
[9] D. A. Malyshev, Y. J. Seo, P. Ordoukhanian, F. E. Romesberg, *J. Am. Chem. Soc.* **2009**, *131*, 14620–14621.
[10] S. Matsuda, J. D. Fillo, A. A. Henry, P. Rai, S. J. Wilkens, T. J. Dwyer, B. H. Geierstanger, D. E. Wemmer, P. G. Schultz, G. Spraggon, F. E. Romesberg, *J. Am. Chem. Soc.* **2007**, *129*, 10466–10473.
[11] S. Matsuda, A. M. Leconte, F. E. Romesberg, *J. Am. Chem. Soc.* **2007**, *129*, 5551–5557.
[12] D. L. McMinn, A. K. Ogawa, Y. Wu, J. Liu, P. G. Schultz, F. E. Romesberg, *J. Am. Chem. Soc.* **1999**, *121*, 11585–11586.
[13] Y. J. Seo, G. T. Hwang, P. Ordoukhanian, F. E. Romesberg, *J. Am. Chem. Soc.* **2009**, *131*, 3246–3252.
[14] Y. J. Seo, S. Matsuda, F. E. Romesberg, *J. Am. Chem. Soc.* **2009**, *131*, 5046–5047.
[15] Y. J. Seo, F. E. Romesberg, *ChemBioChem* **2009**, *10*, 2394–2400.
[16] C. Yu, A. A. Henry, F. E. Romesberg, P. G. Schultz, *Angew. Chem.* **2002**, *114*, 3997–4000; *Angew. Chem. Int. Ed.* **2002**, *41*, 3841–3844.
[17] I. Hirao, *Curr. Opin. Chem. Biol.* **2006**, *10*, 622–627.
[18] I. Hirao, M. Kimoto, T. Mitsui, T. Fujiwara, R. Kawai, A. Sato, Y. Harada, S. Yokoyama, *Nat. Methods* **2006**, *3*, 729–735.
[19] I. Hirao, T. Mitsui, M. Kimoto, S. Yokoyama, *J. Am. Chem. Soc.* **2007**, *129*, 15549–15555.
[20] M. Kimoto, R. Kawai, T. Mitsui, S. Yokoyama, I. Hirao, *Nucleic Acids Res.* **2009**, *37*, e14.
[21] T. Mitsui, A. Kitamura, M. Kimoto, T. To, A. Sato, I. Hirao, S. Yokoyama, *J. Am. Chem. Soc.* **2003**, *125*, 5298–5307.
[22] A. D. Keefe, S. T. Cload, *Curr. Opin. Chem. Biol.* **2008**, *12*, 448–456.
[23] W. Fritzsche, F. Bier, in *International Symposium on DNA-Based Nanodevices*, *Vol. 1062*, American Institute of Physics Conference Proceedings, **2008**.
[24] M. Vrábel, R. Pohl, I. Votruba, M. Sajadi, S. A. Kovalenko, N. P. Ernsting, M. Hocek, *Org. Biomol. Chem.* **2008**, *6*, 2852–2860.
[25] M. A. Wilson, G. Filzen, G. S. Welmaker, *Tetrahedron Lett.* **2009**, *50*, 4807–4809.
[26] J. Ludwig, F. Eckstein, *J. Org. Chem.* **1989**, *54*, 631–635.
[27] M. S. Boosalis, J. Petruska, M. F. Goodman, *J. Biol. Chem.* **1987**, *262*, 14689–14696.
[28] K. Datta, V. J. LiCata, *Nucleic Acids Res.* **2003**, *31*, 5590–5597.
[29] E. Larsen, P. T. Jørgensen, M. A. Sofan, E. B. Pederson, *Synthesis* **1994**, 1037–1038.

Received: July 5, 2011
Published online: December 21, 2011

